



Removal of reactive black 8 dye from aqueous solutions using zinc oxide nanoparticles: investigation of adsorption parameters

Zahra Monsef Khoshhesab^{a,*}, Katayon Gonbadi^a, Gholamreza Rezaei Behbehani^b

^aDepartment of Chemistry, Payame Noor University (PNU), Tehran, Islamic Republic of Iran, emails: monsef_kh@pnu.ac.ir (Z. Monsef Khoshhesab), chemgonbadi@yahoo.com (K. Gonbadi)

^bFaculty of Science, Department of Chemistry, Takestan Branch, Islamic Azad University, Takestan, Islamic Republic of Iran, email: Grb402003@yahoo.com (G. Rezaei Behbehani)

Received 2 March 2014; Accepted 7 September 2014

ABSTRACT

Batch adsorption experiments were carried out to remove reactive black 8 (RB8) from their aqueous solutions using zinc oxide nanoparticles (ZnONPs). The various affecting parameters such as solution pH, contact time, initial dye concentration, and sorbent dosage on the removal efficiency were studied. The equilibrium adsorption data of RB8 on ZnONPs surface were analyzed by Langmuir and Freundlich isotherms. The adsorption process correlated with Langmuir model better than Freundlich isotherm and the maximum adsorption capacity was found to be 27.6 mg g⁻¹. The experimental results showed that the pseudo-second-order kinetic equation could best describe the sorption kinetics.

Keywords: Nanoparticle; Removal; Reactive dyes; Reactive black 8; Zinc oxide

1. Introduction

Growth of population and industrial activities in recent decades cause to enter excessive amount of pollutants to water resources. Among the different types of water pollutants, dyes should be noted as they are extensively used in different industries such as textiles, paper, plastics, leather, food, and cosmetics. The discharge of dyes into wastewaters from coloring industries (particularly the textile industry) is one of the major environmental problems, because it does not only damage the aesthetic natures of the contaminated water, but also disturbs aquatic communities present in the ecosystem by obstructing light penetration and oxygen transfer into water bodies [1]. In addition, some dyes may be degraded into the compounds, having

toxic, mutagenic, and carcinogenic effects on living organisms [2,3]. Therefore, the removal of dyes from industrial wastewaters before being discharged into aquatic systems and environment is very important from health and environmental viewpoints.

Reactive dyes are typically azo-based chromophores combined with different types of reactive groups, e.g. vinyl sulfone, trichloropyrimidine, difluorochloropyrimidine, chlorotriazine, etc. Due to excellent color fastness, bright color, and ease of application, reactive dyes are extensively used in textile industries for dyeing of wool, cotton, nylon, silk, and modified acrylics.

Various physiochemical and biological methods have been developed to treat the dye-containing wastewater [4–12]. However, the chemical and biological stability of the dyestuffs to conventional water treatment make the adsorption technique as an efficient method and more preferable to remove the dyes

*Corresponding author.

from effluents. Several synthetic and natural materials such as clay, activated carbon, polymers, zeolite, and agricultural waste have been developed as adsorbents for treatment of the contaminated waters [13–17]. Activated carbon is one of the most common used adsorbent for water treatment; however, the high cost preparation restricts its extensive applicability [18]. Therefore, researchers have been looking to replace cheaper adsorbents for the activated carbon, providing more efficient results besides the low-cost operation. In recent years, nanostructured materials have attracted extensive attention for adsorption processes because of their high surface area, providing fast kinetics and more efficiency in comparison with the bulk counterparts [19–25].

Zinc oxide (ZnO) is a representative of the metal oxide class which has received considerable attention owing to many of its attractive features such as high photocatalytic activity, the wide band gap of 3.17 eV, nontoxicity, and cost-effective production [26]. At nanoscale, ZnO exhibits electronic, optoelectronic, catalytic, and adsorptive properties. Nanostructures of ZnO are extensively used in optoelectronics, sensors, transducers, cosmetics ingredients, as well as in medicine like dental filling materials, drug carriers, and biosensors [27,28]. ZnO nanostructures have also shown to be nontoxic and biocompatible, suggesting their potential utility in environmental and biological applications [29–31]. Many literatures have used nano-ZnO for the remediation of pollutants in the environment [32–35]. However, most of these researches have been focused on the photocatalytic activity of ZnO and its adsorptive affinity towards various pollutants has been rarely investigated.

In this study, the cauliflower-like ZnO nanoparticles (ZnONPs) have been prepared through a facile precipitation method and used as adsorbent for the reactive black 8 (RB8) removal from aqueous solutions. RB8, an anionic dye, was selected as a model pollutant to investigate the adsorptive properties of the prepared ZnONPs. The affecting parameters such as the initial dye concentration, dye solution pH, adsorbent dosage, and contact time on the adsorption efficiency was investigated. Reaction kinetics and adsorption isotherms were also studied.

2. Experimental

2.1. Materials and equipment

RB8 (Chemical formula: $C_{19}H_{11}ClN_8Na_2O_{10}S_2$, M.W: 656.9 g mol⁻¹) dye was purchased from the Dye-Star Co. (Germany) and used without further purification. Chemical structure of RB8 is presented in Fig. 1. Conventional ZnO powder (approximately 20 μm) was

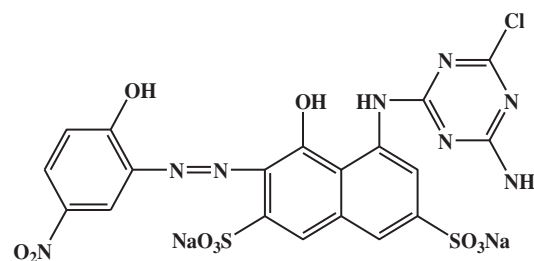


Fig. 1. Chemical structure of RB8.

purchased from Loba Chemie Co. (India). All other reagents and chemicals were of analytical grade and used as received. Double-distilled water was used throughout the experiments for solutions preparation. Stock solution of dye (1,000 mg L⁻¹) was prepared by dissolving an accurately weighed quantity of RB8 in double-distilled water. All of the working solutions were prepared by stepwise dilution of the stock solution with double-distilled water. To adjust the pH of the solutions, NaOH or HCl (0.10 mol L⁻¹) solutions were used.

The prepared ZnONPs were characterized by X-ray diffractometer (XRD; Philips, PW1800) using Cu K_α radiation ($\lambda = 0.15418$ nm, 40 kV, 30 mA), scanning electron microscopy (SEM, Philips XLS30 model), and transmission electron microscopy (TEM, Philips EM208S model). A double-beam UV–vis spectrophotometer (Shimadzu, UV-1601, Japan) with a 1 cm cell was used for measuring the absorption. A Metrohm pH meter (model 827) with a combined glass electrode was used for measuring the pH of solutions. A magnetic stirrer (Heidolph model MR 3001 K) was used for mixing the adsorbent and dye solutions.

2.2. Preparation and characterization of ZnONPs

ZnONPs were prepared from conventional ZnO by precipitation method [36] and used as adsorbent through the adsorption experiments. Briefly, 24 g (0.3 mol) of conventional ZnO powder was added into 100 mL NH₄HCO₃ aqueous solution (48% w/v) under vigorous stirring at 60 °C in two stages: first, 16 g of ZnO was added to the prepared NH₄HCO₃ solution until dissolution was completed (180 min); second, 8 g of ZnO powder and 2 g of CS(NH₂)₂ were sequentially added into the above solution and the mixture was stirred for 2 h at the same temperature. Finally, the resulting slurry was dried at room temperature for 24 h, and then was calcinated at 350 °C for 1 h.

The phase, purity, and the crystallite diameter of the ZnONPs were determined by XRD pattern. The average crystallite size of the ZnO sample was calculated from the diffraction peaks using the Scherrer formula [37]:

$$D_c = \frac{k\lambda}{\beta_{\frac{1}{2}} \cos \theta} \quad (1)$$

where D_c is the crystallite diameter, K is the Scherrer constant (0.89), λ is the X-ray wavelength (0.15418 nm), $\beta_{\frac{1}{2}}$ is the full width at half-maximum intensity of the diffraction peak, and θ is the diffraction angle of the peak.

As shown in Fig. 2, the diffraction peaks appeared at $2\theta = 31.8^\circ, 34.4^\circ, 36.3^\circ, 47.60^\circ, 56.6^\circ, 62.8^\circ, 67.9^\circ,$ and 69.1° are in consistent with the characteristic peaks of the hexagonal wurtzite structure of ZnO (JCPDS card 36-1451). No additional feature related to impurity phase was seen. The average crystallite size, estimated using Scherrer formula was found to be 10 nm. Fig. 3 shows the TEM image of the synthesized ZnONPs, confirming the formation of ZnO nanoparticles with an average size about 9 nm. The particles are in the range of 4–17 nm. Also, the SEM image shows the cauliflower-shaped particles (Fig. 4).

2.3. Batch adsorption experiments

To investigate the potential of ZnONPs for the removal of RB8 dye, a certain amount of the adsorbent was added into 25 mL of the dye solution containing dye with a certain concentration, and the resulting suspension was magnetically stirred (150 rpm) at room temperature ($25^\circ\text{C} \pm 1$). After appropriate time, the adsorbent was removed by filtration and the filtrates were analyzed for the residual concentration of RB8 dye. The concentration of dye in the solution was determined from the calibration curve prepared by measuring different predetermined concentrations of RB8 solutions at a wavelength corresponding to maximum absorbance of RB8 ($\lambda_{\text{max}} = 332 \text{ nm}$) using UV–vis spectrophotometer. The adsorption percent (removal efficiency, R) and adsorption capacity (q_e) were calculated using Eqs. (2) and (3), respectively:

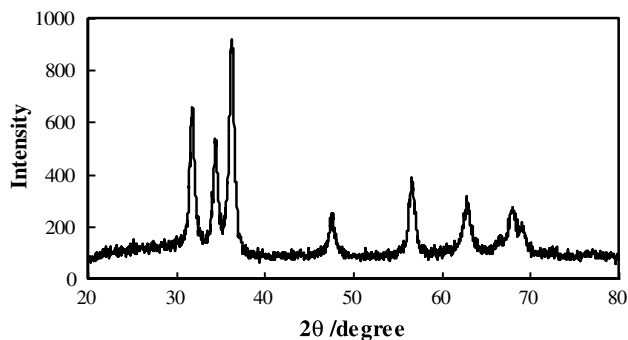


Fig. 2. The XRD pattern of the prepared ZnONPs.

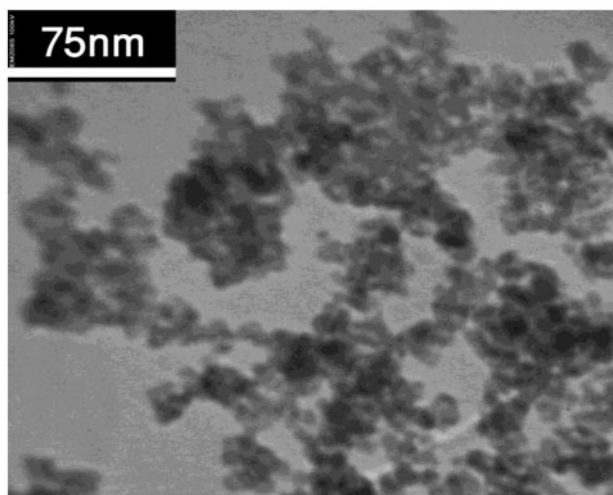


Fig. 3. The TEM image of the prepared ZnONPs.

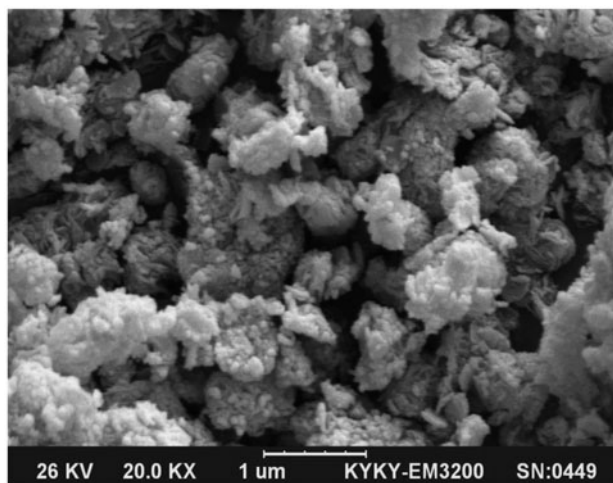


Fig. 4. The SEM image of the prepared ZnONPs.

$$R = \frac{C_0 - C_t}{C_0} \times 100 \quad (2)$$

$$q_e = \frac{(C_0 - C_e) \times V}{m} \quad (3)$$

where C_0 is the initial concentration (mg L^{-1}) of dye and C_t is the concentration of dye after a certain period of time (mg L^{-1}); q_e is the adsorption capacity (mg g^{-1}); V is the volume of RB8 solution (L); and m is the mass of ZnONPs (g).

To determine the maximum amount of adsorption capacity, the impact of various affecting parameters on removal efficiency of the dye by the adsorbent was studied. For this purpose, one parameter was changed

while the other conditions were kept constant. Therefore, the effect of the initial solution pH (3–9), the adsorbent dosage (0.01–0.4 g), initial dye concentration (10–500 mg L⁻¹), and contact time (5–120 min) were studied at room temperature (25°C). In all experiments, the concentration of dye before and after exposure to the adsorbent was calculated using the calibration curve. Also, percentage of the dye removal (*R*) and adsorption capacity (*q_e*) were calculated using Eqs. (2) and (3), respectively. The adsorption kinetics and adsorption isotherms were also performed using a thermostatic bath at constant temperature of 25°C (±0.5). To study the adsorption kinetics of RB8 onto ZnONPs, 0.20 g of the adsorbent was added into 25 mL of 75 mg L⁻¹ RB8 solutions, and the suspensions were agitated for different times. The suspensions were then filtrated and the dye concentration in each supernatant solution was determined. Adsorption isotherm studies were also conducted by mixing 0.2 g of ZnONPs with 25 mL of the dye solutions of different concentrations varying from 10 to 500 mg L⁻¹ (pH 8) for 60 min of agitation time. The suspensions were filtrated and the residual dye concentration in each supernatant solution was determined using UV–vis spectrophotometer. To ensure the repeatability of the results, all experiments were carried out in triplicate and the mean values are presented.

3. Results and discussion

3.1. Effect of the initial pH on the removal efficiency

The effect of the initial pH of the dye solution on the adsorption of RB8 by ZnONPs was evaluated at different solution pHs, ranging from 3 to 9. As shown in Fig. 5, the maximum of the dye removal occurred at pH ~8, and there are no significant changes in the removal efficiency beyond this pH. The effect of pH on the adsorption of RB8 on ZnONPs surface can be mainly explained in terms of electrostatic interactions between the adsorbent surface and the anionic dye species. As it is reported [38], the pH of zero point charge (pH_{ZPC}) of nanosized ZnO particles is around 9, and hence the predominant charge on the ZnONPs surfaces is positive at pHs < 9. Since RB8 has sulfonate (–SO₃) groups in its structure, it can be easily adsorbed onto the ZnO surface (positively charged) through the negative sulfonate groups (at pHs < 9). In addition, in alkaline solutions, deprotonation of hydroxyl groups of phenolic rings in the RB8 molecule can lead to form the anionic phenoxide groups which can be adsorbed onto the ZnONPs surface. Thus, the more adsorption of RB8 at pH 8 may be attributed to the formation of negative phenoxide groups. On the

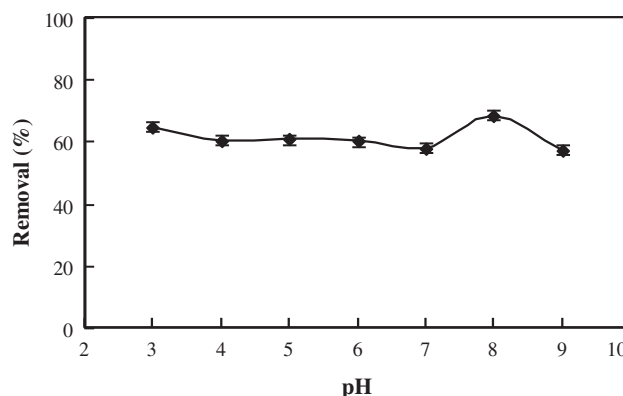


Fig. 5. Effect of pH on the removal efficiency of RB8 by ZnONPs.

Note: Adsorbent dosage: 0.05 g; initial dye concentration: 75 mg L⁻¹; and contact time: 15 min.

other hand, the lower adsorption of the dye at more alkaline pH, may be due to the presence of excess OH⁻ ions that compete with anionic dye molecules for the adsorption sites of adsorbent.

However, the observation of an efficient adsorption at pH 9 as well as other ranges of pHs, suggests that in addition to ionic electrostatic attractions, other adsorption mechanism such as hydrogen bonding may be involved. ZnONPs has no net charge on its surface at pH 9 (the isoelectric point of ZnO); thus, the adsorption process is probably governed by hydrogen bonding occurring between ZnONPs and the amino (or hydroxyl) groups of the RB8 molecule. Such interactions are also expected to take place at all ranges of pH solutions. A similar behavior has been reported for the removal of congo red and methyl orange by ZnO [32,39].

3.2. The effect of contact time on the removal efficiency

The effect of contact time on the adsorption efficiency of RB8 by ZnONPs are presented in Fig. 6. As it can be seen, the adsorption rate was initially high and gradually decreased, and after 60 min, the removal efficiency did not change significantly. This behavior indicates that the kinetics of dye adsorption onto the adsorbent is relatively fast, and about 60% of the dye is removed within the first 5 min of contact time. The high rate of dye adsorption in the beginning and its gradual decrease indicates that there are certain sites on the adsorbent surface. The free sites on the adsorbent surface are decreased as the adsorption of the dye molecules are increased; therefore, there are no empty sites for the adsorption of the remaining dye molecules in solution. Based on the results, a

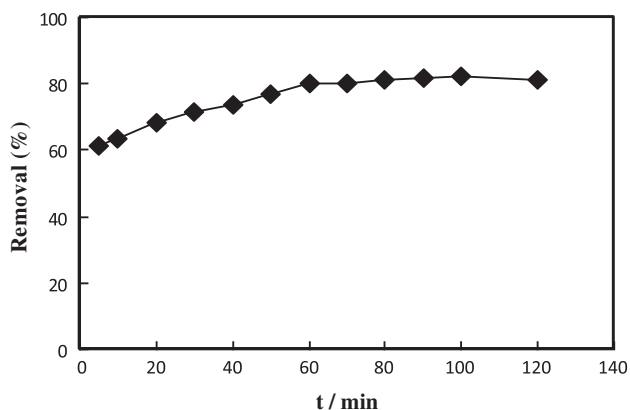


Fig. 6. Effect of contact time on the removal efficiency of RB8 by ZnONPs.
Note: Adsorbent dosage: 0.05 g; initial dye concentration: 75 mg L⁻¹; and pH 8.

contact time of 60 min would be the optimum time for contacting the adsorbent with the dye solution.

3.3. Effect of adsorbent dose on the dye removal efficiency

The influence of the adsorbent dosage on the removal of RB8 by ZnONPs was studied by treating different dosages of adsorbent (0.01–0.4 g) with 25 mL of RB8 (75 mg L⁻¹) solutions at the optimal pH (pH 8) and time (60 min). As it is clear in Fig. 7, the removal percentage of dye increased with the increase in the adsorbent mass and reached the maximum value with 0.2 g of the adsorbent. No significant change was observed with further increase in the adsorbent

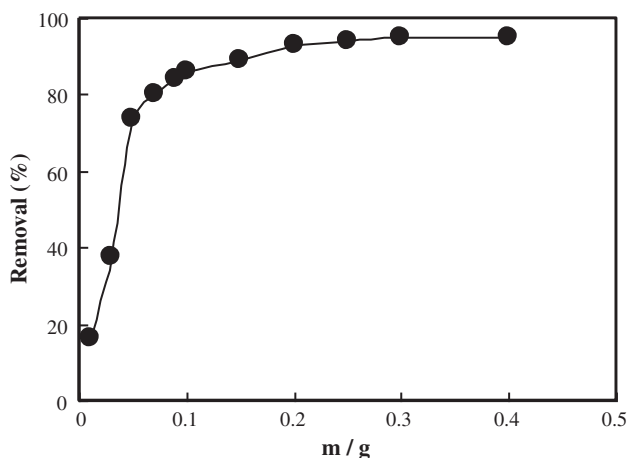


Fig. 7. Effect of adsorbent dosage on the removal of RB8 by ZnONPs.
Note: Initial dye concentration; 75 mg L⁻¹; contact time 60 min, and pH 8.

dosages. Thus, 0.2 g of adsorbent was found as optimum dosage. The increase in the dye removal with the adsorbent mass can be related to the rise in the number of adsorption sites.

3.4. Adsorption kinetics

To investigate the mechanism of adsorption process of RB8 on the ZnONPs surface, the data obtained from adsorption kinetic experiments were analyzed using pseudo-first-order (Lagergren model) and pseudo-second-order kinetic models [40,41], which are expressed by Eqs. (4) and (5), respectively:

$$q_t = q_e[1 - \exp(-k_1 t)] \quad (4)$$

$$q_t = \frac{(k_2 \cdot q_e^2 \cdot t)}{(1 + q_e \cdot k_2 \cdot t)} \quad (5)$$

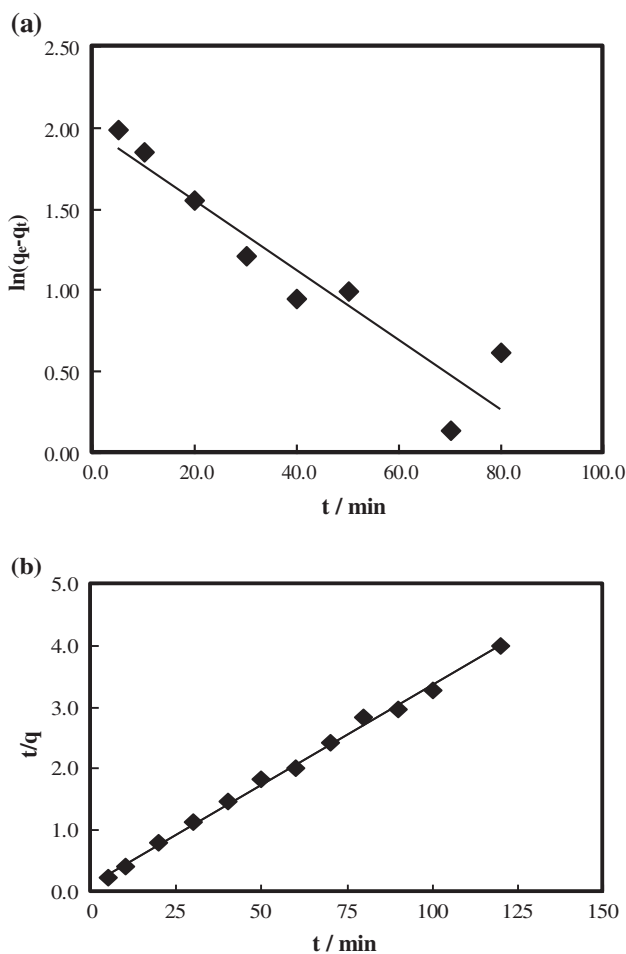


Fig. 8. Pseudo-first-order (a) and pseudo-second-order (b) kinetic plots of RB8 adsorption onto ZnONPs.

Table 1
Pseudo-second-order kinetic parameters of RB8 adsorption onto ZnONPs

Pseudo-first-order parameters				Pseudo-second-order parameters		
q_e (exp) (mg g ⁻¹)	k_1 (min ⁻¹)	q_e (cal) (mg g ⁻¹)	R^2	k_2 (g mg ⁻¹ min ⁻¹)	q_e (cal) (mg g ⁻¹)	R^2
30	0.0215	7.26	0.883	0.0078	31	0.997

where k_1 (min⁻¹) and k_2 (g mg⁻¹ min⁻¹) are the pseudo-first-order and pseudo-second-order rate constants, respectively, q_e and q_t (mg g⁻¹) are the amounts of dye adsorbed at equilibrium and at any time t (min), respectively. For boundary conditions of $q_t=0$ at $t=0$ and $q_t=q_e$ at $t=t_e$, the linear form of the pseudo-first-order equation is expressed as follows:

$$\ln(q_e - q_t) = \ln q_e - k_1 t \quad (6)$$

The k_1 and q_e values can be determined from the slope and intercept of plot $\ln(q_e - q_t)$ vs. $\ln q_e$, respectively. The linear form of the pseudo-second-order kinetic model is represented as:

$$\frac{t}{q_t} = \frac{1}{k_2 q_e^2} + \frac{t}{q_e} \quad (7)$$

The intercept and slope of plot t/q vs. t should give the values of k_2 and q_e , respectively. As shown in Fig. 8, the experimental data fitted to the pseudo-second-order rate better than the pseudo-first-order model. The correlation coefficient (R^2) and the kinetic parameters of the selected kinetic models are listed in Table 1. Good agreement between the experimental q_e ($q_{e,exp}$) and the calculated q_e ($q_{e,cal}$) values as well as the correlation coefficient ($R^2=0.997$) of the pseudo-second-order model, indicating that the adsorption of RB8 onto the ZnONPs can be described by the pseudo-second-order model more appropriately than the pseudo-first-order kinetics. The good agreement between the experimental and calculated data using Eq. (7) demonstrates that the adsorption mechanism depends on the adsorbent and adsorbate, and the rate-limiting step may be chemisorption on a homogenous surface.

3.5. Adsorption isotherms

The adsorption density of the RB8 dye on the ZnONPs surface against the equilibrium concentration of the dye at 25°C is presented in Fig. 9. The equilibrium adsorption data of RB8 on the ZnONPs surface

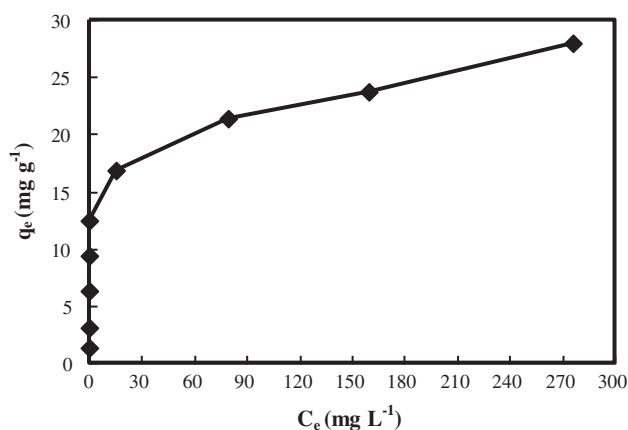


Fig. 9. Adsorption isotherm of RB8 onto ZnONPs at 25°C.

were analyzed using Langmuir and Freundlich isotherms [42,43]. The Langmuir model assumes monolayer adsorption on a uniform surface with a finite number of adsorption sites, while the Freundlich isotherm is applicable to both monolayer (chemisorption) and multilayer adsorption (physisorption), and suitable for nonideal sorption on the heterogeneous surface. The Langmuir and Freundlich isotherms are expressed by Eqs. (8) and (9), respectively:

$$\frac{C_e}{q_e} = \frac{1}{K_L q_m} + \frac{C_e}{q_m} \quad (8)$$

$$\ln q_e = \frac{1}{n} \ln C_e + \ln K_f \quad (9)$$

where q_m is the monolayer adsorption capacity (mg g⁻¹), K_L is the Langmuir adsorption constant which is related to the affinity of the dye molecules for the binding sites (L mg⁻¹) of adsorbent, K_f (mg^(1-1/n) L^{1/n} g⁻¹), and n parameters are the Freundlich adsorption constants which refer to adsorption capacity and adsorption intensity, respectively. The adsorption parameters of the Langmuir and Freundlich isotherms, were determined from the plots of C_e/q_e vs. C_e and $\ln q_e$ vs. $\ln C_e$, respectively.

Table 2
Adsorption isotherm parameters of RB8 onto ZnONPs at 25 °C

Langmuir model				Freundlich model		
q_{\max} (mg g ⁻¹)	K_L (L mg ⁻¹)	R_L	R^2	K_F (mg ^(1-1/n) L ^{1/n} g ⁻¹)	n	R^2
27.6	0.189	0.010	0.991	11.62	6.65	0.953

The obtained results are reported in Table 2. The higher correlation coefficient (R^2) of the Langmuir model indicates that the adsorption process followed the Langmuir model better than the Freundlich isotherm. These results suggest the monolayer adsorption of the RB8 dye on the homogeneous of the ZnONPs surface.

The adsorption process of RB8 onto ZnONPs was also evaluated by Vermeulen criteria associated with the Langmuir isotherm [44,45]. The Vermeulen criteria can be expressed in terms of a dimensionless constant, R_L , called the separation factor that is given by:

$$R_L = \frac{1}{1 + K_L C_0} \quad (10)$$

where K_L (L mg⁻¹) signifies the Langmuir constant and C_0 is the highest initial dye concentration in solution (mg L⁻¹). The value of R_L indicates the adsorption process is unfavorable ($R_L > 1$), linear ($R_L = 1$), favorable ($0 < R_L < 1$), or irreversible ($R_L = 0$). As shown in Table 2, the calculated value of R_L lie between 0 and 1 (0.010) which indicates that the adsorption of RB8 on ZnONPs surface is favorable.

4. Conclusion

The potential use of ZnO nanoparticles, prepared by a facile and low-cost process, for the removal of RB8 from aqueous solutions was investigated. The results showed that the maximum percentage of the dye removal occurred at pH 8 and contact time of 60 min. The kinetic data fitted very well to pseudo-second-order kinetic model. The experimental data were analyzed using Langmuir and Freundlich isotherm models, and the Langmuir model provided the best fit. Therefore, ZnO nanoparticles can be suggested as a biocompatible adsorbent for the removal of RB8 from aqueous solutions, especially textile effluents.

Acknowledgment

The authors gratefully acknowledge the financial and technical support provided by the Payame Noor University.

References

- [1] M. Siddique, R. Farooq, A. Shaheen, Removal of reactive blue 19 from wastewaters by physicochemical and biological processes—A Review, *J. Chem. Soc. Pak.* 33 (2011) 284–293.
- [2] H. Zollinger, *Color Chemistry Synthesis, Properties and Applications of Organic Dyes and Pigments*, VCH Publications, Weinheim, 1991.
- [3] Z. Eren, F.N. Acar, Adsorption of reactive black 5 from an aqueous solution: Equilibrium and kinetic studies, *Desalination* 194 (2006) 1–10.
- [4] D.J. Joo, W.S. Shin, J.H. Choi, S.J. Choi, M.C. Kim, M.H. Han, T.W. Ha, Y.H. Kim, Decolorization of reactive dyes using inorganic coagulants and synthetic polymer, *Dyes Pigm.* 73 (2007) 59–64.
- [5] V. Golob, A. Vinder, M. Simonic, Efficiency of the coagulation/flocculation method for the treatment of dyebath effluents, *Dyes Pigm.* 67 (2005) 93–97.
- [6] M. Koch, A. Yediler, D. Lienert, G. Insel, A. Kettrup, Ozonation of hydrolyzed azo dye reactive yellow 84 (CI), *Chemosphere* 46 (2002) 109–113.
- [7] P.K. Malik, S.K. Saha, Oxidation of direct dyes with hydrogen peroxide using ferrous ion as catalyst, *Sep. Sci. Technol.* 31 (2003) 241–250.
- [8] D.S. Ibrahim, A. Praveen Anand, A. Muthukrishnaraj, R. Thilakavathi, N. Balasubramanian, *In situ* electrocatalytic treatment of a reactive golden yellow HER synthetic dye effluent, *J. Environ. Chem. Eng.* 1 (2013) 2–8.
- [9] M. Visa, L. Andronic, D. Lucaci, A. Duta, Concurrent dyes adsorption and photo-degradation on fly ash based substrates, *Adsorption* 17 (2011) 101–108.
- [10] M. Belhachemi, F. Addoun, Adsorption of congo red onto activated carbons having different surface properties: Studies of kinetics and adsorption equilibrium, *Desalin. Water Treat.* 37 (2012) 122–129.
- [11] M.A.M. Salleh, D.K. Mahmoud, W.A.W.A. Karim, A. Idris, Cationic and anionic dye adsorption by agricultural solid wastes: A comprehensive review, *Desalination* 280 (2011) 1–13.
- [12] B. Royer, N.F. Cardoso, E.C. Lima, T.R. Macedo, C. Airoidi, Sodic and acidic crystalline lamellar magadiite adsorbents for the removal of methylene blue from aqueous solutions: Kinetic and equilibrium studies, *Sep. Sci. Technol.* 45 (2010) 129–141.
- [13] S. Selvakumar, R. Manivasagan, K. Chinnappan, Biodegradation and decolourization of textile dye wastewater using *Ganoderma lucidum*, *Biotech.* 3 (2013) 71–79.
- [14] L.H. Ai, Y. Zhou, J. Jiang, Removal of methylene blue from aqueous solution by montmorillonite/CoFe₂O₄ composite with magnetic separation performance, *Desalination* 266 (2011) 72–77.

- [15] R. Ansari, Z. Mosayebzadeh, Removal of basic dye methylene blue from aqueous solutions using sawdust and sawdust coated with polypyrrole, *J. Iran. Chem. Soc.* 7 (2010) 339–350.
- [16] S.B. Wang, H.T. Li, L.Y. Xu, Application of zeolite MCM-22 for basic dye removal from wastewater, *J. Colloid Interface Sci.* 295 (2006) 71–78.
- [17] M. Hasan, A.L. Ahmad, B.H. Hameed, Adsorption of reactive dye onto cross-linked chitosan/oil palm ash composite beads, *Chem. Eng. J.* 136 (2008) 164–172.
- [18] S. Karaca, A. Gürses, M. Açıkyıldız, M. Ejder (Korucu), Adsorption of cationic dye from aqueous solutions by activated carbon, *Microporous Mesoporous Mater.* 115 (2008) 376–382.
- [19] C.C. Chen, H.J. Fan, J.L. Jan, Degradation pathways and efficiencies of acid blue 1 by photocatalytic reaction with ZnO nanopowder, *J. Phys. Chem. C* 112 (2008) 11962–11972.
- [20] C. Chompuchan, T. Satapanajaru, P. Suntornchot, P. Pengthamkeerati, Decolorization of reactive black 5 and reactive red 198 using nanoscale zerovalent iron, *Int. J. Civ. Environ. Eng.* 2–3 (2010) 123–127.
- [21] G. Moussavi, M. Mahmoudi, Removal of azo and anthraquinone reactive dyes from industrial wastewaters using MgO nanoparticles, *J. Hazard. Mater.* 168 (2009) 806–812.
- [22] J. Hu, Z. Song, L. Chen, H. Yang, J. Li, R. Richards, Adsorption properties of MgO(111) nanoplates for the dye pollutants from wastewater, *J. Chem. Eng. Data* 55 (2010) 3742–3748.
- [23] T. Madrakian, A. Afkhami, N. Rezvani Jalal, M. Ahmadi, Kinetic and thermodynamic studies of the adsorption of several anionic dyes from water samples on magnetite-modified multi-walled carbon nanotubes, *Sep. Sci. Technol.* 48 (2013) 2638–2648.
- [24] B. Saha, S. Das, J. Saikia, G. Das, Preferential and enhanced adsorption of different dyes on iron oxide nanoparticles: A comparative study, *J. Phys. Chem. C* 115 (2011) 8024–8033.
- [25] B. Cheng, Y. Le, W. Cai, J. Yu, Synthesis of hierarchical Ni(OH)₂ and NiO nanosheets and their adsorption kinetics and isotherms to congo red in water, *J. Hazard. Mater.* 185 (2011) 889–897.
- [26] Q. Zhang, K. Yu, W. Bai, Q. Wang, F. Xu, Z. Zhu, N. Dai, Y. Sun, Synthesis, optical and field emission properties of three different ZnO nanostructures, *Mater. Lett.* 61 (2007) 3890–3892.
- [27] P. Jiang, J.J. Zhou, H.F. Fang, C.Y. Wang, Z.L. Wang, S.S. Xie, Hierarchical shelled ZnO structures made of bunched nanowire arrays, *Adv. Funct. Mater.* 17 (2007) 1303–1310.
- [28] I.T. Degim, D. Kadioglu, Cheap, suitable, predictable and manageable nanoparticles for drug delivery: Quantum dots, *Curr. Drug Deliv.* 10 (2013) 32–38.
- [29] J. Zhou, N. Xu, Z.L. Wang, Dissolving behavior and stability of ZnO wires in biofluids: A study on biodegradability and biocompatibility of ZnO nanostructures, *Adv. Mater.* 18 (2006) 2432–2435.
- [30] Z. Li, R. Yang, M. Yu, F. Bai, C. Li, Z.L. Wang, Cellular level biocompatibility and biosafety of ZnO nanowires, *J. Phys. Chem. C* 112 (2008) 20114–20117.
- [31] R. Gopikrishnan, K. Zhang, P. Ravichandran, S. Baluchamy, V. Ramesh, S. Biradar, P. Ramesh, J. Pradhan, J.C. Hall, A.K. Pradhan, G.T. Ramesh, Synthesis, characterization and biocompatibility studies of zinc oxide (ZnO) nanorods for biomedical application, *Nano-Micro Lett.* 2 (2010) 31–36.
- [32] M. Movahedi, A.R. Mahjoub, S. Janitabar-Darzi, Photodegradation of congo red in aqueous solution on ZnO as an alternative catalyst to TiO₂, *J. Iran. Chem. Soc.* 6 (2009) 570–577.
- [33] K. Melghit, M.S. Al-Rubaei, I. Al-Amri, Photodegradation enhancement of Congo red aqueous solution using a mixture of SnO₂·xH₂O gel/ZnO powder, *J. Photochem. Photobiol., A* 181 (2006) 137–141.
- [34] C. Lizama, J. Freer, J. Baeza, H.D. Mansilla, Optimized photodegradation of reactive blue 19 on TiO₂ and ZnO suspensions, *Catal. Today* 76 (2002) 235–246.
- [35] R. Velmurugan, K. Selvam, B. Krishnakumar, M. Swaminathan, An efficient reusable and antiphotocorrosive nano ZnO for the mineralization of Reactive Orange 4 under UV-A light, *Sep. Purif. Technol.* 80 (2011) 119–124.
- [36] Z. Monsef Khoshhesab, M. Sarfaraz, M. Asadi Asadabad, Preparation of ZnO nanostructures by chemical precipitation method, *Synth. React. Inorg. Met.-Org. Nano-Met. Chem.* 41 (2011) 814–819.
- [37] B.D. Cullity, *Elements of X-ray Diffraction*, third ed., Addison-Wesley, Reading, MA, 1967.
- [38] E. Topoglidis, A.E.G. Cass, B. O'Regan, J.R. Durrant, Immobilisation and bioelectrochemistry of proteins nanoporous TiO₂ and ZnO Films, *J. Electroanal. Chem.* 517 (2001) 20–27.
- [39] C. Chen, J. Liu, P. Liu, B. Yu, Investigation of photocatalytic degradation of methyl orange by using nano-sized ZnO catalysts, *Adv. Chem. Eng. Sci.* 1 (2011) 9–14.
- [40] S. Lagergren, About the theory of so-called adsorption of soluble substances, *Kung. Sven. Vetén. Hand.* 24 (1898) 1–39.
- [41] Y.S. Ho, G. McKay, Pseudo-second order model for sorption processes, *Process Biochem.* 34 (1999) 451–465.
- [42] I. Langmuir, The adsorption of gases on plane surfaces of glass, mica and platinum, *J. Am. Chem. Soc.* 40 (1918) 1361–1403.
- [43] H.M.F. Freundlich, Over the adsorption in solution, *J. Phys. Chem.* 57 (1906) 385–471.
- [44] L. Ai, M. Li, L. Li, Adsorption of methylene blue from aqueous solution with activated carbon/cobalt ferrite/alginate composite beads: Kinetics, isotherms, and thermodynamics, *J. Chem. Eng. Data* 56 (2011) 3475–3483.
- [45] T.W. Weber, R.K. Chakravorti, Pore and solid diffusion models for fixed-bed adsorbers, *AIChE J.* 20 (1974) 228–238.